Energy-Based Approach for the Analysis of a Vertically Loaded Pile in Multi-layered Non-linear Soil Strata

Prakash Ankitha Arvan (parvan2018@fau.edu)
Florida Atlantic University https://orcid.org/0000-0002-8573-2061
Madasamy Arockiasamy
Florida Atlantic University

Research Article

Keywords: Piles, Multi-layered soil, Soil non-linearity, Analytical solutions, Vertical (Axial) load, Pile displacement, MATLAB R2019a, ANSYS 2019R3

Posted Date: November 30th, 2021

DOI: https://doi.org/10.21203/rs.3.rs-337774/v1

Energy-based Approach for the Analysis of a Vertically Loaded Pile in Multi-layered Non-linear Soil Strata

Arvan Prakash Ankitha[1], M. ASCE, Madasamy Arockiasamy[2], PhD., P.E., P.Eng., F. ASCE

[1] Doctoral Research Scholar, Department of Civil, Environmental and Geomatics Engineering, Florida Atlantic University, Boca Raton, FL 33431-0991, USA. Email: parvan2018@fau.edu

ORCID: 0000-0002-8573-2061

[2]Professor and Director, Center for Infrastructure and Constructed Facilities, Department of Civil, Environmental and Geomatics Engineering, Florida Atlantic University, Boca Raton, FL 33431-0991, USA. Email: arockias@fau.edu

ORCID: 0000-0002-0249-7394

Abstract

Numerous studies have been reported in published literature on analytical solutions for a vertically loaded pile installed in a homogeneous single soil layer. However, piles are rarely installed in an ideal homogeneous single soil layer. This study presents an energy-based approach to obtain displacements in an axially loaded pile embedded in multi-layered soil considering soil non-linearity. A simple power law based on published literature is used where the soil is assumed to be nonlinear-elastic and perfectly plastic. A Tresca yield surface is assumed to develop the soil stiffness variation with different strain levels that defines the non-linearity of the soil strata. The pile displacement response is obtained using the software MATLAB R2019a and the results from the energy-based method are compared with those obtained from the field test data as well as the finite element analysis based on the software ANSYS 2019R3. It is observed that the results obtained from the energy-based method are in better agreement with the field measured values than those obtained from the FEA. The approach presented in this study can be extended to piles embedded in multi-layered soil strata subjected to different cases of lateral loads as well as the combined action of lateral and axial loads. Furthermore, the same approach can be extended to study the response of the soil to group piles.

Keywords

Piles; Multi-layered soil; Soil non-linearity; Analytical solutions; Vertical (Axial) load; Pile displacement; MATLAB R2019a; ANSYS 2019R3.

Declarations

Funding Not applicable

Conflicts of interest/Competing interests Not applicable

Availability of data and material Not applicable

Code availability Not applicable

Author's contributions Not applicable

Acknowledgements

The authors acknowledge the support received from the Florida Department of Transportation Grant: DOT-RFP-20-9069-CA and Florida Atlantic University for providing the senior author with the Presidential Fellowship to successfully finish this study.

1 Introduction

Many studies are available in the literature that explains the pile deformation response under different loading conditions with the pile embedded in multi-layered soil, which treat the soil as linear elastic. However, for practical applications to the real world, it is important to study the response of the non-linear behavior of the soil and the variation of soil stiffness based on its stress and strain levels. A discretized continuum approach (numerical method) or the energy-based method is preferred over the beam-on-elastic foundation approach since the approach considers the surrounding soil behavior in three dimensions: vertical, radial and circumferential directions. Several researchers estimated the pile deformations based on the energy-based method [Poulos 1971a, Poulos 1971b, Banerjee and Davies 1978, 16, Basack and Dey 2012, Georgiadis et al. 2013, Verrujit and koojiman 1989, Basu et al. 2008]. There are many numerical methods available in the published literature with various pile geometry and constitutive models using Finite Element Method [Randolph 1981, Brown et al. 1989, Trochanis et al. 1991, Carter and Kulhawy 1992, Bransby and Springman 1996, Bransby 1999]; Finite Difference Method [Ng and Zhang 2001, Klar and Frydman 2002, Basu et al. 2008, Basu et al. 2008, Haldar and Babu 2012]; and Boundary Element Method [Banerjee and Davies 1978,

Budhu and Davies 1988, Basack and Dey 2011, Basack and Dey 2012]. The present study is based on the Finite Difference method since it yields results faster when compared to the Finite Element Method.

Linear Elastic Soil Model

An analytical solution based on the energy-based method was used by several researchers [Vlasov and Leont'ev 1966, Vallabhan and Das 1991a, Basu and Salgado 2007, Basu et al. 2008, Basu et al. 2008, Basu et al. 2009, Seo and Prezzi 2007, Seo et al. 2009] to estimate laterally loaded and axially loaded pile deformation for linear elastic soil. Independent functions describing the soil displacement have been used; these functions vary in vertical, radial and circumferential directions. The linear elastic analysis has been developed by employing variational principles and minimization of energy, called Hamilton's principle, to derive the governing equation and boundary conditions. Hamilton's equation can be expressed as

$$\int_{t_1}^{t_2}(\delta T - \delta U)dt + \int_{t_1}^{t_2}\delta W\, dt \qquad (1)$$

where T and U are the kinetic and potential energies of the pile and soil and W is the work done by the applied load, t_1 and t_2 are the initial and final times of loading [Asik and Vallaban 2001].

The governing equations for pile deflection are obtained by minimizing kinetic and potential energies. These governing equations can be solved either numerically or analytically for a given set of boundary conditions. Each of the displacement components are expressed as a multiplication of one-dimensional functions when minimizing the energy to obtain a set of one-dimensional equation. These equations are solved numerically using the finite difference technique. In these studies, the soil is treated as linear elastic where the shear modulus G and the Lame's constant λ are treated as constants for all the layers [Fidel 2014].

Constitutive Model for Non-Linear Soil Behavior

In order to consider the non-linear effect of soil, the soil moduli G and λ are assumed to vary in radial, circumferential and vertical directions according to the strain and stress levels [Basu et al. 2008]. The stress and strain decay with increasing distances in the radial direction accomapnied by an increase in soil stiffness G. In other words, soil stiffness degrades with increasing strain and hence it varies in both radial and vertical directions. The analysis of the soil behavior using a single constitutive model is very idealistic since the undrained strength of soil depends on a number

of factors such as the soil anisotropy, failure mode, strain rate, stress paths and the mode of loading effects of stress-strain non-linearity which make the undrained strength dependent on the test type [Koutsoftas and Ladd 1985, Kulhawy and Mayne 1990]. Consideration of the non-linear soil behavior will be more realistic in the analysis of pile displacement response. For piles subjected to external loads, the decay of the soil stiffness varies with strain which in turn depends on the type of the soil. The stiffness of soil was high at a very small strain level and decreases with the increase in the strain [Atkinson 2000]. Many reasearchers [Jardine et al. 1984, Burland 1990, Atkinson and Sallfors 1991, Houlsby and Wroth 1991, Osman et al. 2007, Osman et al. 2007] conducted triaxial tests and reported high values of soil stiffness when the shear strains are less than 10^{-5}. Several factors including the mean effective stress, void ratio, stress history, rate of loading, soil plasticity for silts and clays, stress anisotropy for sands and the effective confining stress affect the small strain stiffness G_{max} [Frnevich and Massarsch 1979, Hardin and Drnevich 1972, Hardin 1978, Presti et al. 1996, Vucetic 1994, Yamashita et al. 2003]. The decay of the soil stiffness with the increase of strain levels can be defined using the power law [Bolton and Whittle 1999, Bolton et al. 1993, Gunn 1992].

This paper presents an energy-based approach to study the displacement profile of a vertically loaded pile in multi-layered soil strata considering the soil non-linear behavior. A simple power law is used by Gunn [Gunn 1993] where the soil is assumed to be nonlinear-elastic and perfectly plastic. A Tresca yield surface is assumed to develop the soil stiffness variation with different strain levels that defines the non-linearity of the soil strata. The pile displacement response is obtained using the software MATLAB R2019a. The results from the energy-based method are compared with those from the field test data as well as the finite element analysis based on the software ANSYS 2019R3. The results from the energy-based method are in good agreement with both the field test data and the finite element analysis.

2 Problem Definition

An axially loaded pile in an isotropic non-linear elastic multilayered soil medium is shown in Fig. 1. This study considers a pile of length L with circular cross section of radius r_0. The pile is embedded in n horizontal soil layers and is subjected to an axial (vertical) load P_t. The horizontal soil layers extend to infinity in the radial direction and the bottom n^{th} layer extends to infinity in the vertical direction.

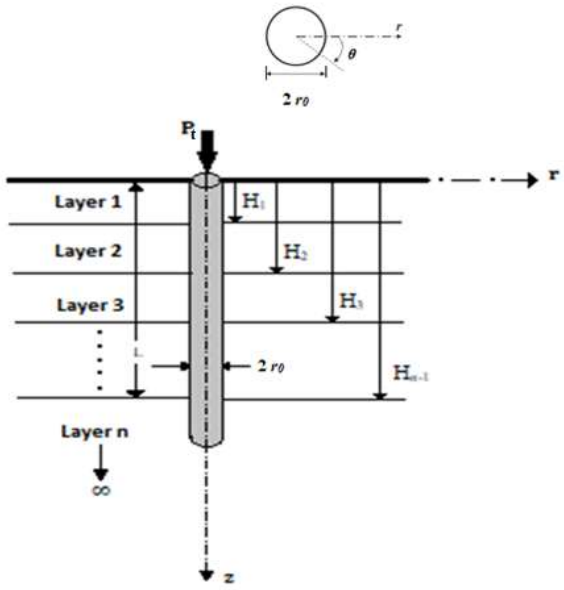

Fig. 1 An axially loaded pile in an isotropic nonlinear elastic medium

The terms $H_1, H_2, H_3 \ldots H_{n-1}$ denote the vertical height from the ground surface to the bottom of any layer i. Therefore, the thickness of any layer i is $H_i - H_{i-1}$ with $H_0 = 0$. Due to the axisymmetric problem behavior, a system of cylindrical coordinates (r-θ- z) is chosen with the origin coinciding with the center of the pile cross section at the pile head and the z axis coinciding with the pile axis. The pile head is considered to be free and the tip of the pile is clamped. Another important assumption to be noted is that there is no slippage or separation between the pile and the surrounding soil and between soil layers. The stresses and the displacement within a soil continuum are shown below in Fig. 2 (a) and (b).

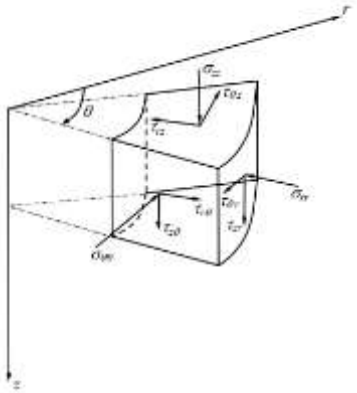

(a) Stresses within a soil continuum

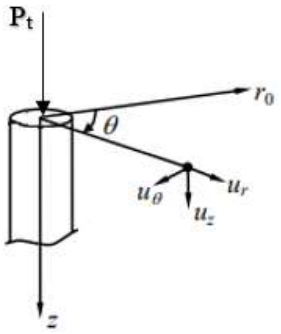

(b) Displacement within a soil continuum

Fig. 2 Stresses and displacements within a soil continuum

At each point in the soil domain, G and λ have been calculated (Fig. 3).

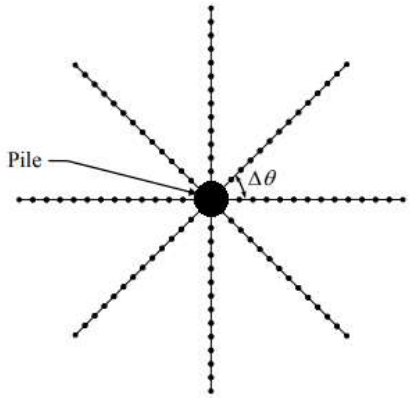

(a) Plan

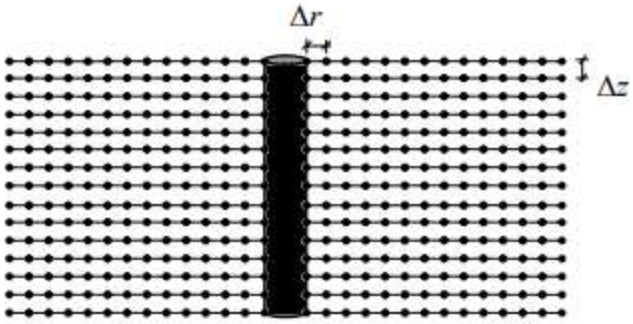

(b) Elevation

Fig. 3 Discretization of the soil (adapted from Basu et al. 2008)

The goal of the analysis is to obtain pile head deflection caused by the action of the vertical load P_t at the pile head.

2.1 Basic assumptions of an axially loaded pile in multi-layered soil

For an axially loaded pile, the horizontal and tangential displacements can be neglected as they are accompanied by very small strains [Salgado et al. 2007]. For the case of a pile with circular cross-section there are two functions to be considered: $v(z)$ which will represent the vertical displacement at depth z and the dimensionless functions $\phi(r)$ describing the variation of soil displacements in the radial direction.

The vertical displacement at any point of the soil is represented as a function in (r, z):

$$v_r = 0 \tag{2}$$

$$v_\theta = 0 \tag{3}$$

$$v_z(r,z) = \phi(r)v(z) \tag{4}$$

For a given uniform cross-sectional area of the pile along the length, $\phi(r) = 1$ when $r = 0$ to r_0, while $\phi(r) = 0$ when $r \rightarrow \infty$. This explains the decay of the function $\phi(r)$ with an increase in the radial direction.

Governing Differential Equation

The pile and its surrounding elastic medium are subjected to a vertical displacement of the pile soil system when it is acted upon by a vertical load. The total potential energy of the pile and the soil is a summation of internal potential energy and external potential energy [Basu et al. 2008], which is given as:

$$\Pi = \frac{1}{2} E_p A_p \int_0^L \left(\phi \frac{dv}{dz}\right)^2 dz + \frac{1}{2} \int_0^L \int_0^{2\pi} \int_{r_0}^{\infty} \sigma_{ij}\varepsilon_{ij} r dr d\theta dz + \frac{1}{2} \int_L^{\infty} \int_0^{2\pi} \int_0^{\infty} \sigma_{ij}\varepsilon_{ij} dr - vP_{t\ at\ z=0} \tag{5}$$

Where E_p denotes the elastic Young modulus of the pile, A_p denotes the cross-section of the pile, v represents the vertical displacement, P_t is the vertical load and σ_{ij}, ε_{ij} are stress and strain components respectively. The first term of the equation represents potential pile energy, the second and third terms are potential energy from the surrounding soil and the soil below the pile respectively.

The soil non-linearity is considered by varying the soil elastic parameters (G and λ) at each discretized nodal point in the soil domain. The stress-strain and strain-displacement relationships at any given nodal point in the soil medium are idealized by the following relationships. The stress-strain relationship is expressed as:

$$\begin{bmatrix}\boldsymbol{\sigma_r}\\ \boldsymbol{\sigma_\theta}\\ \boldsymbol{\sigma_z}\\ \boldsymbol{\tau_{r\theta}}\\ \boldsymbol{\tau_{rz}}\\ \boldsymbol{\tau_{\theta z}}\end{bmatrix} = \begin{bmatrix}\boldsymbol{\lambda+2G} & \boldsymbol{\lambda} & \boldsymbol{\lambda} & \boldsymbol{0} & \boldsymbol{0} & \boldsymbol{0}\\ \boldsymbol{\lambda} & \boldsymbol{\lambda+2G} & \boldsymbol{\lambda} & \boldsymbol{0} & \boldsymbol{0} & \boldsymbol{0}\\ \boldsymbol{\lambda} & \boldsymbol{\lambda} & \boldsymbol{\lambda+2G} & \boldsymbol{0} & \boldsymbol{0} & \boldsymbol{0}\\ \boldsymbol{0} & \boldsymbol{0} & \boldsymbol{0} & \boldsymbol{G} & \boldsymbol{0} & \boldsymbol{0}\\ \boldsymbol{0} & \boldsymbol{0} & \boldsymbol{0} & \boldsymbol{0} & \boldsymbol{G} & \boldsymbol{0}\\ \boldsymbol{0} & \boldsymbol{0} & \boldsymbol{0} & \boldsymbol{0} & \boldsymbol{0} & \boldsymbol{G}\end{bmatrix}\begin{bmatrix}\boldsymbol{\varepsilon_r}\\ \boldsymbol{\varepsilon_\theta}\\ \boldsymbol{\varepsilon_z}\\ \boldsymbol{\gamma_{r\theta}}\\ \boldsymbol{\gamma_{rz}}\\ \boldsymbol{\gamma_{\theta z}}\end{bmatrix} \tag{6}$$

where G and λ are the elastic constants of the soil. The strain-displacement relationship is given by:

$$\begin{bmatrix}\boldsymbol{\varepsilon_r}\\ \boldsymbol{\varepsilon_\theta}\\ \boldsymbol{\varepsilon_z}\\ \boldsymbol{\gamma_{r\theta}}\\ \boldsymbol{\gamma_{rz}}\\ \boldsymbol{\gamma_{\theta z}}\end{bmatrix} = \begin{bmatrix}-\frac{\partial \mathbf{u_r}}{\partial \mathbf{r}}\\ -\frac{\boldsymbol{u_r}}{\boldsymbol{r}}-\frac{\mathbf{1}}{\boldsymbol{r}}\frac{\partial \mathbf{u_\theta}}{\partial \boldsymbol{\theta}}\\ -\frac{\partial \mathbf{u_z}}{\partial \mathbf{z}}\\ -\frac{\mathbf{1}}{\boldsymbol{r}}\frac{\partial \mathbf{u_r}}{\partial \boldsymbol{\theta}}-\frac{\partial \mathbf{u_\theta}}{\partial \mathbf{r}}+\frac{\boldsymbol{u_\theta}}{\boldsymbol{r}}\\ -\frac{\partial \mathbf{u_z}}{\partial \mathbf{r}}-\frac{\partial \mathbf{u_r}}{\partial \mathbf{z}}\\ -\frac{\mathbf{1}}{\boldsymbol{r}}\frac{\partial \mathbf{u_z}}{\partial \boldsymbol{\theta}}-\frac{\partial \mathbf{u_\theta}}{\partial \mathbf{z}}\end{bmatrix} = \begin{bmatrix}\mathbf{0}\\ \mathbf{0}\\ -\boldsymbol{\phi}(\boldsymbol{r})\frac{\boldsymbol{dv(z)}}{\boldsymbol{dz}}\\ \mathbf{0}\\ -\boldsymbol{v}(\boldsymbol{z})\frac{\boldsymbol{d\phi(r)}}{\boldsymbol{dr}}\\ \mathbf{0}\end{bmatrix} \tag{7}$$

By substituting Equation (7) into Equation (6), the strain energy density function $W = \frac{\sigma_{ij}\varepsilon_{ij}}{2}$ is obtained, where the summation implies the repetition of the indices i and j as required in indicial notation:

$$\tfrac{1}{2}\sigma_{ij}\varepsilon_{ij} = \tfrac{1}{2}\left[(\lambda+2G)\left(\phi\tfrac{dv}{dz}\right)^2 + G\left(v\tfrac{d\phi}{dr}\right)^2\right] \tag{8}$$

Substituting Equation (8) into Equation (5) and integrating with respect to θ, the potential energy equation becomes:

$$\Pi = \tfrac{1}{2}\,E_pA_p\int_0^L\left(\phi\tfrac{dv}{dz}\right)^2\,dz + \pi\int_0^L\int_{r_o}^{\infty}\left((\lambda+2G)\left(\phi\tfrac{dv}{dz}\right)^2 + G\left(v\tfrac{d\phi}{dr}\right)^2\right)rdrdz + \pi\int_L^{\infty}\int_0^{\infty}\Big((\lambda+2G)\left(\phi\tfrac{dv}{dz}\right)^2 + G\left(v\tfrac{d\phi}{dr}\right)^2\Big)rdrdz - vP_{t\ at\ z=0} \tag{9}$$

The variational principle has been used to calculate the potential energy δU and the external energy δW [Vallabhan and Mustafa 1996, Lee and Xiao 1999]. As a result, the governing equations of the pile-soil system are obtained by minimizing the potential energy of soil and pile. The expression of potential energy contains different functions, such as $v(z)$, $\phi(r)$, $\frac{dv(z)}{dz}$ and $\frac{d\phi(r)}{dr}$, so by minimizing the potential energy gives

$$\delta\Pi = \left[A(v)\delta v + B(v)\delta\left(\frac{dv}{dz}\right)\right] + [C(\phi)\delta\phi] \tag{10}$$

where A, B and C are the terms associated with variations δv, $\delta\left(\frac{dv}{dz}\right)$ and $\delta\phi$.

The variation of equation (9) becomes

$$\delta\Pi = \frac{1}{2} E_p A_p \int_0^L \phi \frac{dv}{dz} \delta\phi \frac{dv}{dz} dz + \pi \int_0^L \int_{r_o}^{\infty} \left((\lambda + 2G)(\phi \frac{dv}{dz} \delta\phi \frac{dv}{dz}) + G(v \frac{d\phi}{dr} \delta v \frac{d\phi}{dr}) \right) r dr dz + \pi \int_L^{\infty} \int_0^{\infty} \left((\lambda + 2G)(\phi \frac{dv}{dz} \delta\phi \frac{dv}{dz}) + G(v \frac{d\phi}{dr} \delta v \frac{d\phi}{dr}) \right) r dr dz - v P_{t\ at\ (z=0)} \quad (11)$$

Output Parameters

(i) Pile Displacement

The governing equation of the pile is obtained for $0 < z < L$ by collecting terms associated with $\delta v dz$, $\delta \frac{dv}{dz} dz$ and its derivative, δv and $\delta \frac{dv}{dz} dz \neq 0$. The governing equation is obtained as follows:

$$k \frac{d^2 v}{dz^2} + C \frac{dv}{dz} + mv = 0 \quad (12)$$

where

$$C = 2\pi \int_{r_0}^{\infty} r \left[(\lambda + 2G) \phi^2 \right] dr \quad (13)$$

$$k = E_p I_p + 2\pi \int_{r_0}^{\infty} r \left[(\lambda + 2G) \phi^2 \right] dr \quad (14)$$

$$m = -2\pi \int_{r_0}^{\infty} rG \left(\frac{d\phi}{dr} \right)^2 dr \quad (15)$$

For this study, the tip of a pile is assumed to be clamped, which means that the displacement and the curvature are equal to zero at the base of the pile. The boundary conditions are obtained by collecting δv and $\delta \frac{dv}{dz}$. At the head of the pile ($z = 0$):

$$-E_p A_p - 2\pi \int_{r_0}^{\infty} r \left[\lambda + G(2 + \phi^2) \right] dr \frac{dv}{dz} + P_t = 0 \quad (16)$$

The displacement at the tip of the pile ($z=L$):

$$v = 0 \quad (17)$$

The second order differential equation (12) can be solved using a central finite difference scheme. Equation (12) becomes

$$k\left(\frac{v_{i-1}-2v_i+v_{i+1}}{\Delta z^2}\right)+C\left(\frac{v_{i-1}+v_{i+1}}{\Delta z}\right)+mv_i=0 \quad (18)$$

where i denotes the i^{th} node in z direction, and Δz is the distance between two nodes. This discretized analysis is then solved using the software MATLAB R2019a.

(ii) Soil Displacement

The governing equation of the soil is obtained for $r_0 \leq r \leq \infty$ by collecting terms associated with $\delta\phi dr$:

$$r\frac{d^2\phi}{dr^2}+\gamma_1\frac{d\phi}{dr}+\gamma_2\phi=0 \quad (19)$$

where

$$\gamma_1=\frac{\int_0^L G+rG}{\int_0^L G} \quad (20)$$

$$\gamma_2=\frac{-\int_0^L(\lambda+2G)\left(\frac{dv}{dz}\right)^2}{\int_0^L G\,v^2} \quad (21)$$

Similar to the solution of Equation (12) by the central finite difference scheme, the governing differential equation (19) is also solved using the finite difference method (using the software MATLAB R2019a).

2.2 Soil non-linearity

The variation of the shear stress with strain can be described using two parameters A and n that have been obtained experimentally using a pressuremeter test as shown in the equation below:

$$q=A\left(\varepsilon_q\right)^n \quad (22)$$

Where q represents the equivalent shear stress, ε_q is the deviator shear strain. Atkinson (2000) shows that the decay curves of the soil stiffness with strain can be divided into three regions as shown in Fig. 4. The first region in Fig. 4 represents the very small strain where the stiffness, G_0 is constant, the second region comprising small strains starts from ε_0 till $\varepsilon = 0.1\%$ and the third region exceeds $\varepsilon = 0.1\%$ indicative of large strains.

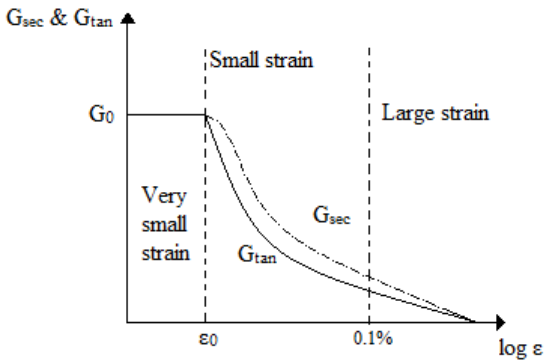

198

199 **Fig. 4** The variation of normalizing shear secant with logarithmic strain ε_q or normalized displacement (adapted from Atkinson, 2000)

200 In the second region the stiffness decays rapidly and in the third region with large strain levels, the stiffness is the
201 smallest, which concludes that the soil stiffness is high at small strain and decreases with large strain [Atkinson 2000].
202 Fig. 5 shows the degradation of soil stiffness with increasing strains for different clay types.

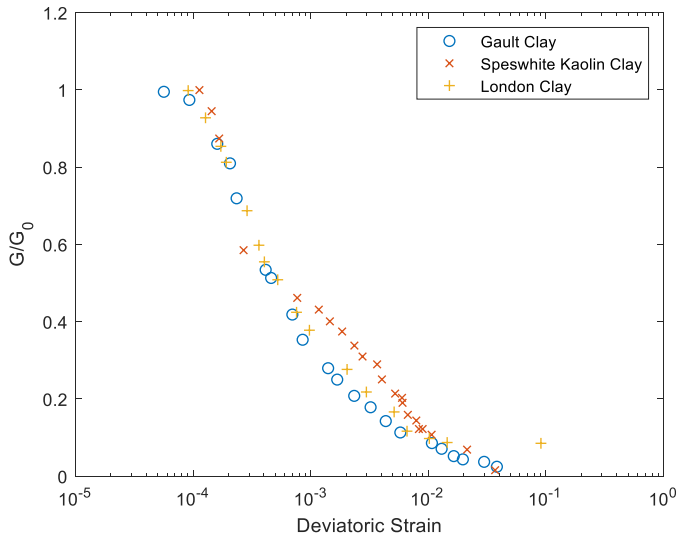

203

204 **Fig. 5** Degradation of tangent with deviatoric strain (Adapted from Dasari [19])

205 The present study assumes decay of soil stiffness with strain using a power law to describe the stress-strain behaviour
206 of soil [Gunn 1993, Bolton and Whittle 1999]:

207 $$G = G_0 \left(\frac{\varepsilon_q}{\varepsilon_{q0}}\right)^n \tag{23}$$

208 $$G = a\, \varepsilon_q^n \tag{24}$$

where $a = \frac{G_0}{\varepsilon q_0^n}$, is a constant determined empirically, n describes soil nonlinearity which is equal to *(-0.5)* according to the experimental data analyzed by Osman et al. (2007) (Fig. 6). ε_q represents the deviatoric strain and ε_{q_0} is the maximum deviatoric strain with linear elastic behavior which is equal to 10^{-5}. The soil stiffness G is estimated by calculating strain at each location followed by the power law.

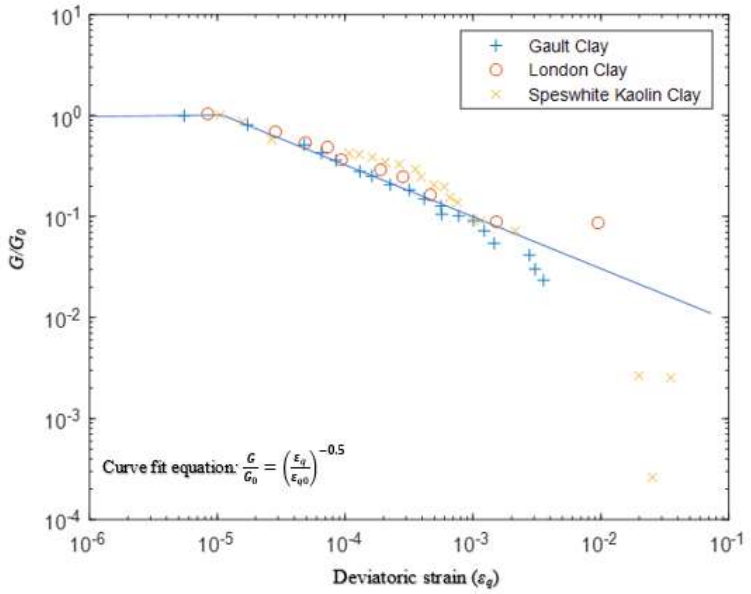

Fig. 6 Logarithmic scale of degradation of tangent stiffness with strain level (Adapted from Osman et al. 2007 after Dasari 1996)

3 Iterative Solution Methodology

The pile deflection equation can be solved when the soil and geometry related parameters k, C and m are known; however, these parameters depend on the unknown dimensionless soil function ϕ, which can be estimated by calculating γ_1 and γ_2. Soil displacement is obtained when the initial numbers of these values γ_1 and γ_2, are inserted into Equation 19, from which the parameters k, C and m are obtained as a result of the pile displacement. New values of γ_1 and γ_2 (Equations (20) and (21)) are determined and then inserted into Equation 19 to evaluate ϕ, then v, so an iteration technique is needed to obtain the condition $\frac{\gamma_{old}-\gamma_{new}}{\gamma_{old}} > 0.001$. This iterative solution methodology (Fig. 7) is used as input to the software MATLAB R2019a to obtain the pile head displacements.

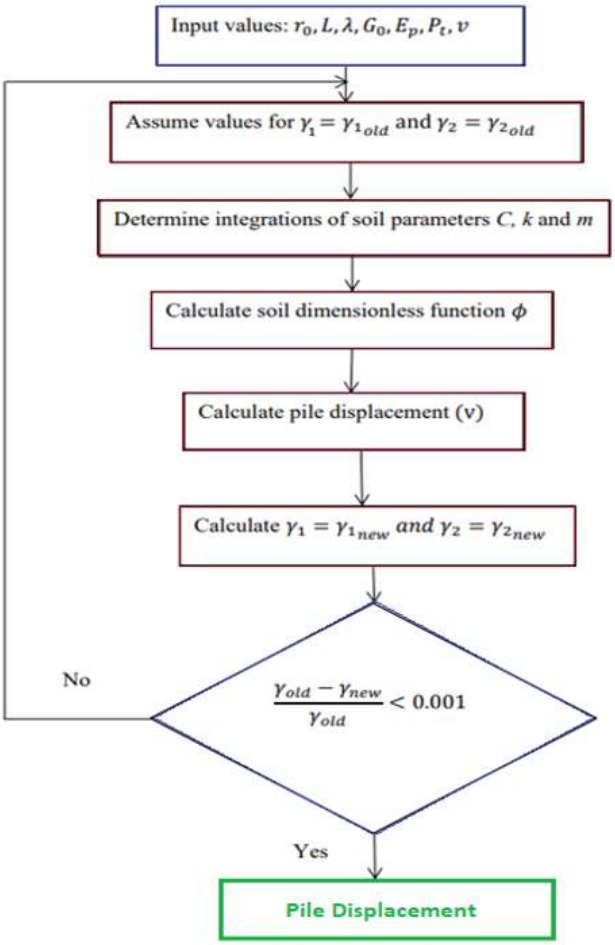

Fig. 7 Flowchart of the iterative solution scheme

(Adapted from Fidel 2014 after Basu et al. 2008)

4 Validation based on both Field Test Data and Finite Element Analysis (FEA) using ANSYS 2019 R3

Field Test Data

(a) "Full-scale load tests on instrumented micropiles": Russo (2004)

The present study makes a comparison of Russo's field test data to validate the superiority of the energy-based method for non-linear elastic soil over the linear elastic solution of Salgado et al. 2007. Russo (2004) outlined the case history of micro piles used for underpinning a historical building in Naples, Italy. A load test was carried out on a micro pile, 0.2 *m* in diameter and 19 *m* in length with an elastic modulus of 27 *GPa*, as shown in Fig. 8. The pile and soil characteristics used in the present study are adopted from the published literature by Seo and Prezzi (2007).

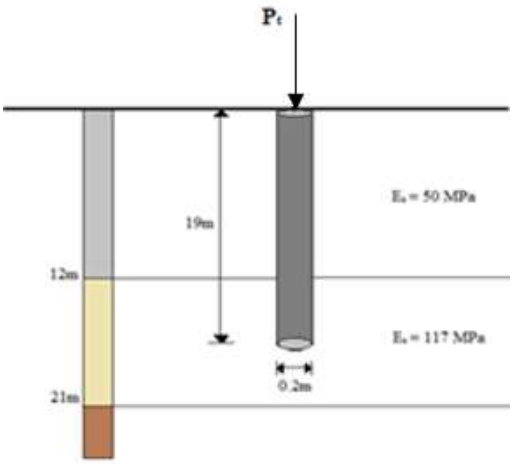

Fig. 8 The soil profile and elastic properties of each layer (adapted from Russo 2004)

The soil characteristics are given below:

Table 1 Soil characteristics at the site

Soil Characteristics	Soil thickness (*m*)	Young's Modulus, *E* (*MPa*)	Shear Modulus, G_0 (*MPa*)	Poisson's Ratio
Layer 1	12	50	35	0.3
Layer 2	9	117	18	0.3

The power law equation (Equation (24)) is used to model the soil stiffness as a function of strain to account for the soil non-linearity. In Equation (24), $a = \frac{G_0}{\varepsilon q_0^n}$, is a constant value and the value of G_0 for each layer is taken as reported from Table 1, ε_q donates deviatoric strain, ε_{q_0} is the maximum deviatoric strain with linear elastic behavior which is equal to 10^{-5} and *n* represents a constant. The present study uses the published data for *n = -0.5* proposed by Osman et al. (2007).

A series of axial loads were applied to the pile head to obtain the corresponding vertical displacements. Fig. 9 compares the pile displacements from the energy-based method with the field data and the linear elastic solution.

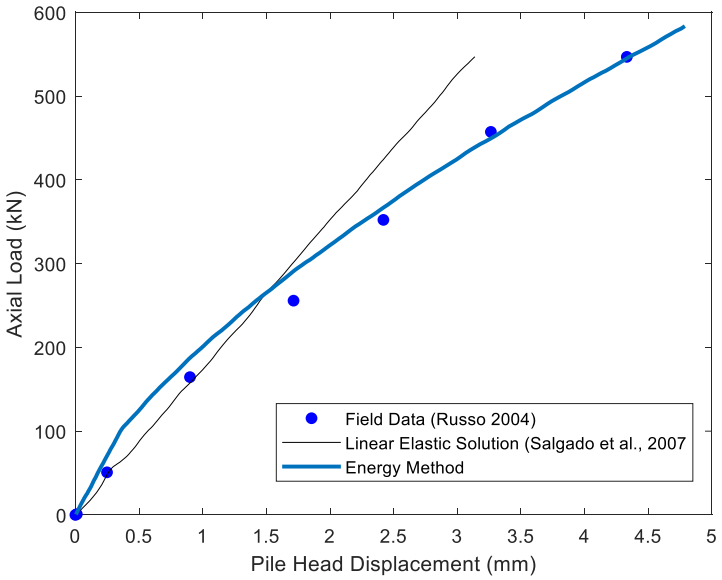

Fig. 9 Response of the pile due to axial load

The predicted pile displacements in the present study are in good agreement with the field data. It can be seen that the pile displacements from the present study and the published field data are greater than the computed values based on linear elastic soil solution when the axial load in the pile exceeds 300 *kN*.

(b) "An instrumented driven pile in Dublin boulder clay": Farrell et al. (1998)

Farrell et al. (1998) conducted field experiments with an instrumented tubular steel pile driven into Dublin boulder clay (DBC). The aim of these experiments, undertaken as a part of a research project at Trinity College Dublin (TCD), was to improve the understanding of the factors governing the axial load capacity of driven piles in hard glacial tills.

Soil Characteristics:

The area's geotechnical characteristics was investigated by various researchers [Skipper et al. 2005, Long and Menkiti 2007, Farrell et al. 1988, Gavin et al. 2008]. The area of the outcrop of the DBC is indicated in Fig. 10 [Long and Menkiti 2007]. The sketch map is not intended to be a definite geological map of Dublin but aims to show the location of the study sites and the prevalence of DBC in the area.

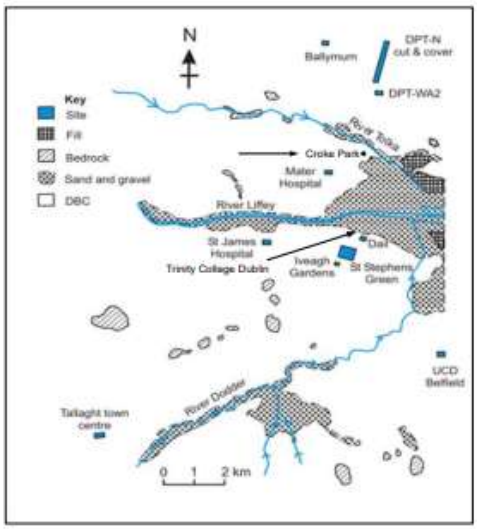

Fig. 10 Location sites in Dublin (Long and Menkiti 2007)

A detailed description of the geology at the test site is given by Skipper et al. (2005) whereas a brief summary is given by Long and Menkiti (2007). The geology of the area as investigated by [Long and Menkiti 2007], classifies the soil layers into four categories: Upper Brown Boulder Clay (UBrBC), Upper Black Dublin Boulder Clay (UBkBC), Lower Brown Dublin Boulder Clay (LBrBC), and Lower Black Dublin Boulder Clay. An undrained triaxial compression test was conducted in order to determine the undrained shear strength of the black boulder clay, which was 450 *kPa*. Moreover, Phillips and Lehane (1998) and Long and Menkiti (2007), determined that the average undrained strength for upper brown boulder clay (UBrBC) was 100 *kPa*, and between 350 *kPa* and 600 *kPa* for upper black boulder clay (UBkBC). In the present study, an average undrained strength of 450 *kPa* was adopted. Lame's constant and shear modulus vary in the nonlinear soil and pile responses are calculated by assuming the soil as homogenous. Long and Menkiti (2007) reported $G_0 = 98$ *MPa* for the first layer and $G_0 = 83$ *MPa* for the second layer. A single 'operational' value of $E_u = 100$ *MPa* is used, as derived from field observations [Farrell et al. 1995a]. The degradations of soil stiffness for UBrBC and UBkBC based on the present study are shown in Fig. 11 and Fig. 12 respectively. The initial soil stiffness used in the calculations is based on Long's study, and also calculated using the power law relation in Equation (24). The present study uses the published data for $n = -0.5$ proposed by Osman et al. (2007). This value is in good agreement with published values for clay by Long and Menkiti (2007).

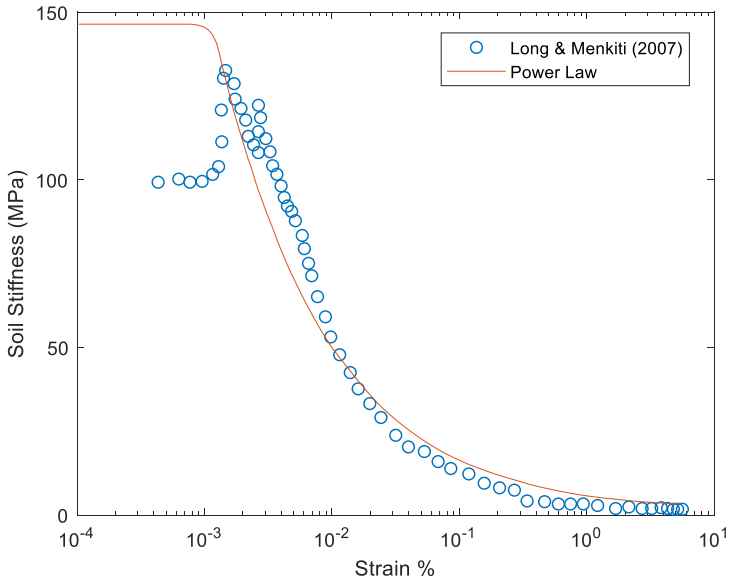

277

278 **Fig. 11** Variation of soil stiffness with strains for Upper Brown Boulder Clay

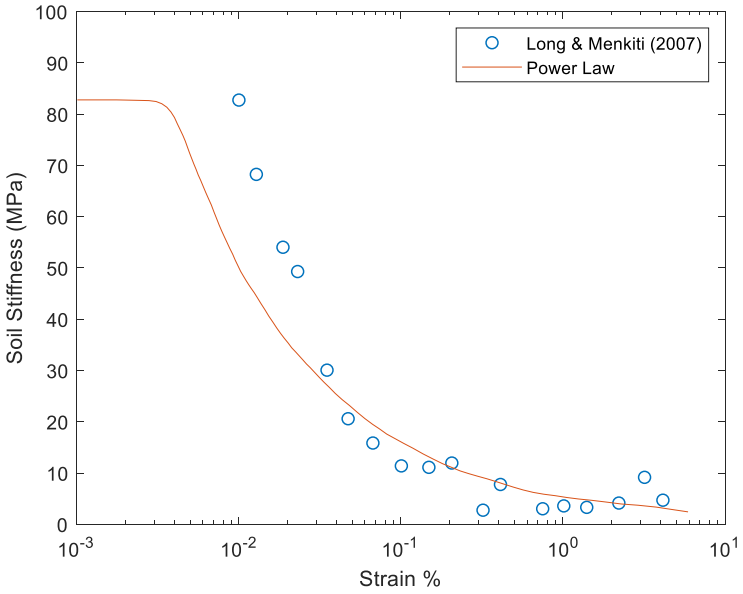

279

280 **Fig. 12** Variation of soil stiffness with strains for Upper Black Boulder Clay

281 Pile Characteristics:

282 A steel closed-end tubular driven pile, 0.273 *m* in diameter and 7.5 *m* in length, was embedded in the boulder clay
283 (Fig.13). The thickness of the pile was 10 *mm* (0.01 *m*) (Fig. 11). A flat 20 *mm* (0.02 *m*) thick, 0.273 *m* diameter steel
284 disc was used to close the pile base.

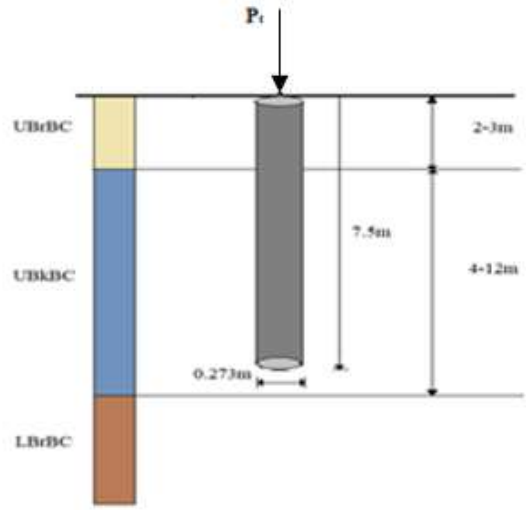

285

286 **Fig. 13** Pile Profile at TCD in Dublin

287 A series of axial loads were applied to the pile in order to obtain the pile-soil deformation. The field test results are
288 then compared with the analytical solutions from the energy-based approach. Fig. 14 shows axial load versus observed
289 and predicted pile head deformations.

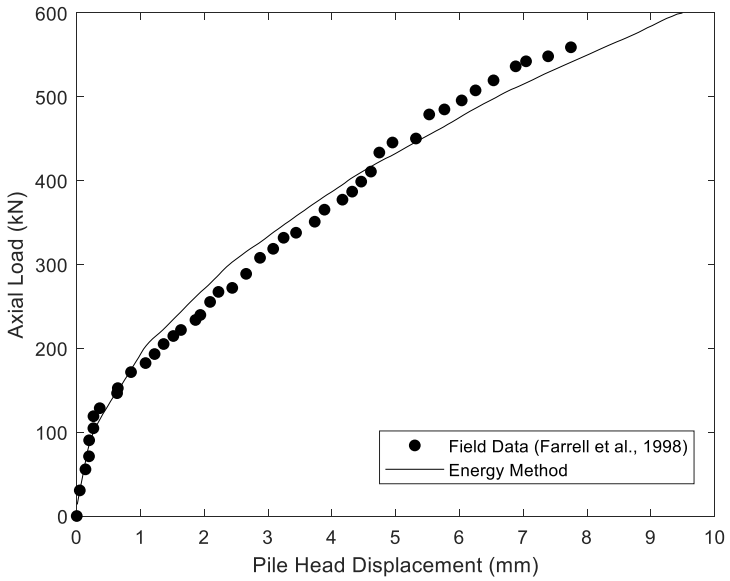

290

291 **Fig. 14** Response of the head of the axially loaded pile

292 Fig. 14 shows that the energy-based method predicts the pile head displacements which are in good agreement with
293 the field measurements.

Finite Element Analysis using ANSYS 2019 R3

A FEA was conducted using the software ANSYS Workbench 2019 R3 for the Soil-Pile problem as discussed in the above section. A static structural analysis was chosen and the input data for the soil characteristics was taken from Long and Menkiti (2007). The pile characteristics were added according to the steel pile used by Farrell et al. (1998). The soil non-linearity was considered based on the actual soil stress-strain curves reported by Long and Menkiti (2007) for each soil layer (as shown in Fig. 15 and Fig. 16).

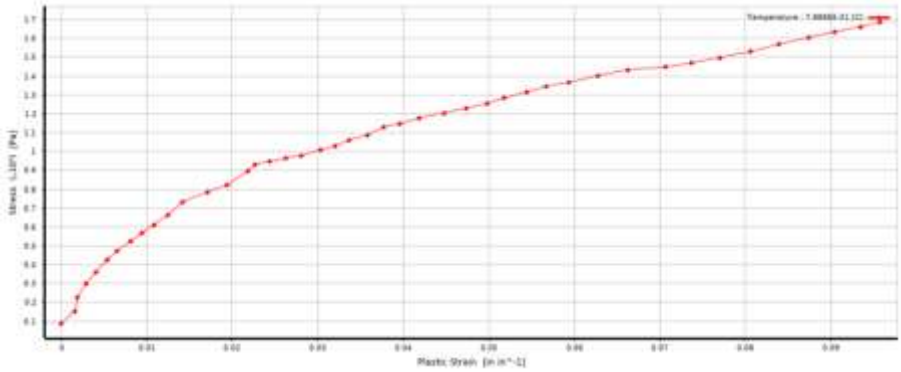

Fig. 15 Input Stress-strain relationship curve of soil layer 1 for the software ANSYS

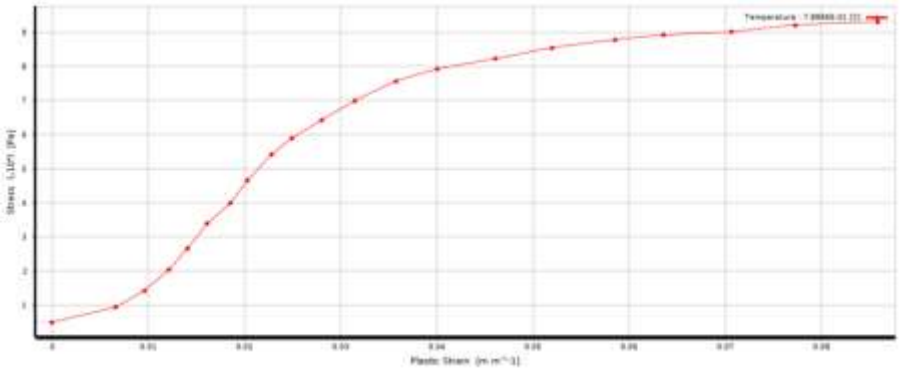

Fig. 16 Input Stress-strain relationship curve of soil layer 2 for the software ANSYS

The soil block's length was chosen as 15 times the pile diameter (15D) and the depth was according to the depth of each soil layer. The soil block was fixed at the bottom and free on the surroundings. The discretized Finite Element Model (FEM) with a coarse mesh of 6978 nodes and 2039 elements is shown in Fig. 17. A Directional Deformation along the *Z*-axis is used to calculate the displacements of pile head for the respective force applied.

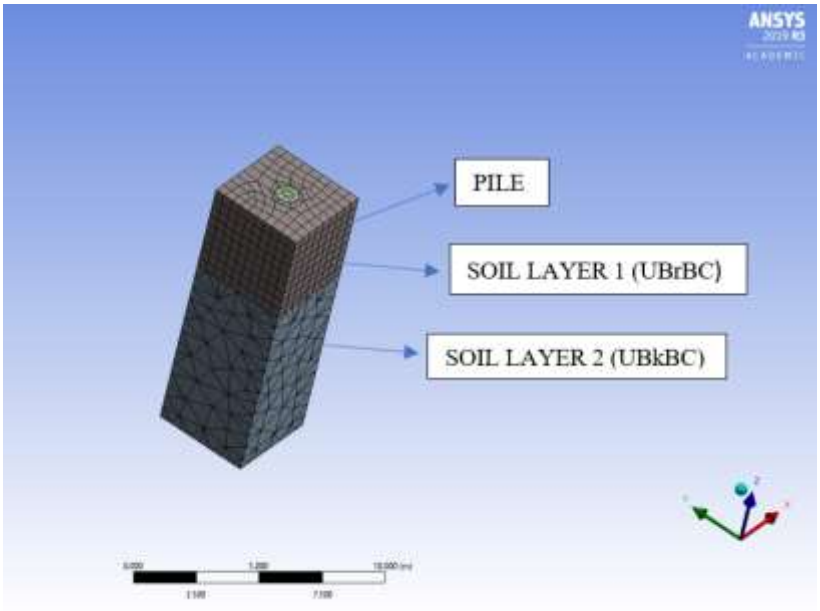

Fig. 17 A mesh representation of the FEM Model (ANSYS 2019 R3)

Fig. 18 compares the pile head displacements obtained by energy-based method and the FEM Analysis. Both the methods underestimate the pile head displacements when compared to the field measured values. However, the displacements obtained by energy-based method are in good agreement upto 20 *kN*. On the other hand, the FEA gives displacements close to field measured values only upto 10 *kN* and beyond that the displacements appear to be smaller.

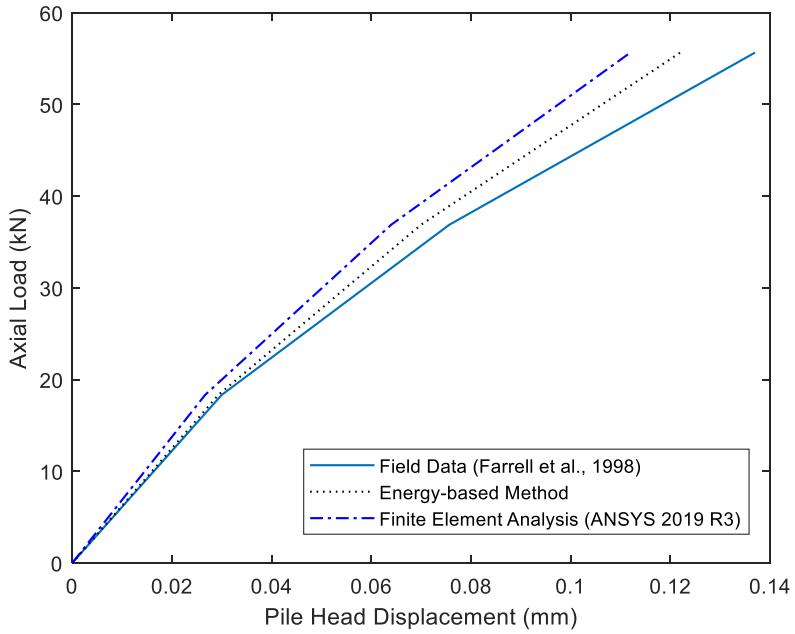

Fig. 18 Pile Displacements resulting from FEM Analysis

5 Discussions

The beam-on-nonlinear-foundation approach (*p-y* method) has been used extensively used to understand the pile-displacement responses. This approach has the limitation of representing the surrounding soil using nonlinear springs requiring realistic user specified soil characteristics of *p-y* curves which do not represent the three-dimensional pile-soil interaction. Several researchers have studied the pile responses using numerical methods including boundary element method, finite element method and finite difference method. Although the finite element method using appropriate soil constitutive relationship, elements and domains for the soil and pile gives realistic results, the method requires enormous computation time and the resources required for such an analysis stands out as a major limitation. This gives rise to the need for a more efficient method which has both the strength of a rigorous three-dimensional nonlinear approach for the pile-soil interaction and potentials for obtaining a faster computational effort. The present study presents an analytical solution based on an energy method (discretized continuum approach) to predict pile soil displacements, where the soil is assumed to be non-linear elastic (soil parameters vary in radial, tangential and vertical directions). The analysis was conducted on an axially (vertical) loaded pile embedded in multilayered soil. Governing equations for pile and soil have been obtained by applying the variational principle to the potential energy which are then solved using the software MATLAB R2019a. Comparisons have been made with the published field data and the finite element method. It is observed that the energy-based method described in this study is in good agreement with the field data when compared to the linear elastic solution that does not consider the soil non-linearity. The FEA has been carried out using the software ANSYS Workbench 2019 R3. The soil non-linearity is considered by inserting the stress-strain curves of each soil layer available from the published literature. It is observed that the results obtained from the energy-based method are in better agreement with the field measured values than those obtained from the FEA. The study illustrates the superior advantage of the fast solutions obtained by the energy-based method over the finite element method.

6 Conclusions and Future work

The present energy-based method considering the non-linear response of the soil gives a good approximation of the field data when compared to the linear elastic solution and the finite element method. The main goal of this study is

to extend the same approach to laterally loaded pile and to the combined action of lateral and axial loading on the pile. Furthermore, the same approach will be extended to study the response of the soil to group piles.

References

1. Asik, M. Z and Vallaban, C. V. G. (2001). A simplified model for the analysis of machine foundations on non-saturated elastic and linear soil layer. Journal of Computers and Structures, 79, pp 2717-2726.
2. Atkinson, J. H and Sallfors, G. (1991). Experimental determination of stress-strain-time characteristics in laboratory and in situ tests. Proceedings of the 10th European Conference on Soil Mechanics and Foundation Engineering, Florence, 3, pp 915-956.
3. Atkinson, J. H. (2000). Non-linear soil stiffness in routine design. Géotechnique, 50 (5), pp 478-508.
4. Banerjee, P. K and Davies, T. G. (1978). The behaviour of axially and laterally loaded single piles embedded in non-homogeneous soils. Géotechnique, 28(3), pp 309-326.
5. Basack, S and Dey, S. (2011). Pile subjected to lateral cycle loading in sand. Proceedings of the Indian Geotechnical Conference. Paper No. N343.
6. Basack, S and Dey, S. (2012). Influence of relative pile-soil stiffness and load eccentricity on single pile response in sand under lateral cyclic loading. Geotechnical and Geological Engineering, an International Journal, springer, 30(2), pp 737-751.
7. Basu, D and Salgado, R. (2007). Elastic analysis of laterally loaded pile in multi-layered soil. Journal of Geomechanics and Geoengineering. 2 (3), pp 183-196.
8. Basu, D., Prezzi, M., Salgado, R and Chakraborty, T. (2008). Settlement analysis of piles with rectangular cross sections in multi-layered soils. Computers and Geotechnics Journal, 35, pp 563-575.
9. Basu, D., Salgado, R and Prezzi, M. (2008). Analysis of laterally loaded piles in multilayered soil deposits. Publication FHWA/IN/JTRP-2008/23. Joint Transportation Research Program, Indiana. Department of Transportation and Purdue University, West Lafayette, Indiana. doi: 10.5703/1288284313454.
10. Basu, D., Salgado, R and Prezzi, M. (2009). A continuum- based model for analysis of laterally loaded piles in layered soils. Géotechnique, 59 (2), pp 127-140.
11. Bolton, M. D and Whittle, R. W. (1999). A non-linear elastic perfectly plastic analysis for plane strain undrained expansion. Géotechnique, 49 (1), pp 133-141.

12. Bolton, M. D., Sun, H. W and Britto, A. M. (1993). Finite element analyses of bridge abutments of firm clay. Computers and Geotechnics Journal, 15, pp 22-245.
13. Bransby, M. F. and Springman, S. M. (1996). 3D finite element modelling of pile groups adjacent to surcharge loads. Journal of Computers and Geotechnics, 19 (4), pp 301-324.
14. Bransby, M. F. (1999). Selection of p–y curves for the design of single laterally loaded piles. International Journal for Numerical and Analytical Methods in Geomechanics, 23(15), pp 1909-1926.
15. Brown, D. A., Shie, C. and Kumar, M. (1989). P–y curves for laterally loaded piles derived from three-dimensional finite element model. Proceeding of the 3rd International Symposium on Numerical Models in Geomechanics (NUMOG III), Niagara Falls, pp 683- 690.
16. Budhu, M and Davies, T. G. (1988). Nonlinear analysis of laterally loaded piles in cohesionless soil. Canadian Geotechnical Journal, 24, pp 289-296.
17. Burland, J. B. (1990). 30th Rankine lecture- on the compressibility and shear-strength of natural clays, Géotechnique, 40(3), ISSN: 0016-8505, pp 329-378.
18. Carter, J. P and Kulhawy, F.H. (1992). Analysis of laterally loaded shafts in rock. Journal of Geotechnical Engineering, 118(6), pp 839-855.
19. Dasari, G. R. (1996). Modelling the variation of soil stiffness during sequential construction. PhD thesis, University of Cambridge.
20. Drnevich, V. P and Massarsch, K. R. (1979). Sample disturbance and stress-strain behavior. ASCE Journal of Geotechnical Engineering Division, 105 (GT9), pp 1001-1016.
21. Farrell, E. R., Bunni, N. G and Mulligan, J. (1988). The bearing capacity of Dublin black boulder clay. Transactions of the Institution of Engineers of Ireland, 112, pp 77-104.
22. Farrell, E. R., Coxon, P., Doff, D. H and Priedhomme, L. (1995a). The genesis of brown boulder clay of Dublin. Quarterly Journal of Engineering Geology, 28, pp 143-152.
23. Farrell, E., Lehane, B and Loopy, M. (1998). An instrumented driven pile in Dublin boulder clay. Journal of the Geotechnical Engineering Division, 131, pp 233-241.
24. Gavin, K., Cadogan, D and Towmey, L. (2008). Axial resistance of CFA piles in Dublin Boulder Clay. Proceeding of the Institution of Civil Engineers, Geotechnical Engineering, 161 (GE4), pp171-180.

25. Georgiadis, K., Sloan, S. W and Lyamin, A. V. (2013). Undrained limiting lateral soil pressure on a row of piles. Journal of Computers and Geotechnics, 54, pp 175-184.
26. Gunn, M. J. (1992). The prediction of surface settlement profiles due to tunnelling. Predictive soil mechanics, Proceedings of the Wroth Memorial Symposium, Oxford, pp 304-316.
27. Gunn, M. J. (1993). The prediction of surface settlement profiles due to tunneling, Predictive soil mechanics, Houlsby and Schofield (eds.), Proceedings of the Wroth Memorial Symposium, Thomas Telford, London, pp 304-314.
28. Haldar, S and Sivakumar Babu, G. L. (2012). Response of vertically loaded pile in clay: a probabilistic study. Journal of Geotechnical and Geological Engineering, 30(1), pp 187- 196.
29. Hardin, B. O and Drnevich, V. P. (1972). Shear modulus and damping in soils: design equations and curves. Journal of the Soil Mechanics and Foundations Division, American Society of Civil Engineers, 98(SM 7), pp 667-692.
30. Hardin, B. O. (1978). The nature of the stress-strain behaviour of soils. Earthquake Engineering and Soil Dynamics, American Society of Civil Engineers, 1, pp 3-9.
31. Hashem-ali, Salma, Fidel (2014) Analytical methods for predicting load-displacement behavior of piles, Durham theses, Durham University. Available at Durham E-Theses Online: http://etheses.dur.ac.uk/10918/
32. Houlsby, G. T and Wroth, C. P. (1991). The variation of shear modulus of a clay with pressure and over consolidation ratio. Journal of Soils and Foundations, 31 (3), pp 138-143.
33. Jardine, R. J., Symes, M. J and Burland, J. B. (1984). The measurement of soil stiffness in the triaxial apparatus. Géotechnique, 34 (3), pp 323-340.
34. Klar, A and Frydman, S. (2002). Three-dimensional analysis of lateral pile response using two-dimensional explicit numerical scheme. Journal of Geotechnical and Geoenvironmental Engineering, American Society of Civil Engineers, 128 (9), pp 775-784.
35. Koutsoftas, D. C and Ladd, C. C. (1985). Design strengths for an offshore clay. Journal of the Soil Mechanics and Foundations Division, American Society of Civil Engineers, 111 (3), pp 337-355.
36. Kulhawy, F. H and Mayne, P. W. (1990). Manual on estimating soil properties for foundation design, Report No. EL-6800, Electric Power Research Institute, Palo Alto, CA.

37. Lee, K-M and Xiao, Z. R. (1999). A new analytical model for settlement analysis of a single pile in multi-layered soil. Journal of Soils and Foundations, 39(5), pp 131-143.
38. Lo Presti, D. C. F., Jamiolkowski, M., Oronzo, P and Cavallaro. (1996). Rate and creep effect on the stiffness of soils. Poceeding of the Measuring and Modeling Time Dependent Soil Behavior, pp 166-180.
39. Long, M and Menkiti, C. O. (2007). Geotechnical properties of Dublin boulder clay. Géotechnique, 57 (7), pp 595-611.
40. Ng, C. W. W and Zhang, L.M. (2001). Three-dimensional analysis of performance of laterally loaded sleeved piles in sloping ground. Journal of Geotechnical and Geoenvironmental Engineering, American Society of Civil Engineers, 127 (6), pp 499-509.
41. Osman, A. S., White, D. J., Britto A. M and Bolton, M. D. (2007). Non-linear displacement of shallow foundations on undrained clay. Géotechnique, 57(9), pp 729-737.
42. Osman, A. S., White, D. J., Britto, A. M and Bolton, M. D (2007). Simple prediction of the undrained displacement of a circular surface foundation on non-linear soil. Géotechnique, 57 (9), pp 729-737.
43. Phillips, D. M and Lehane, B. M. (1998). The lateral capacity of an instrumented pile in glacial till. Proceeding of the VII International Conference on Piling and Deep foundations, Vienna, 5, pp 131-136.
44. Poulos, H. G. (1971 b). Behavior of laterally loaded piles: II pile groups. Journal of the Soil Mechanics and Foundation Division, American Society of Civil Engineers, 97(SM5), pp 733- 751.
45. Poulos, H. G. (1971a). Behavior of laterally loaded piles: I-Single Piles. Journal of the Soil Mechanics and Foundation Division, American Society of Civil Engineers, 97(SM5), pp 711-731.
46. Randolph, M. F. (1981). The response of flexible piles to lateral loading. Géotechnique, 31(2), pp 247-259.
47. Russo, G. (2004). Full-scale load test on instrumented micropiles. Proceedings of the Institution of Civil Engineers: Geotechnical Engineering, 157(3), pp 127-135.
48. Salgado, R., Prezzi, M and Seo, H. (2007). Advanced modeling tools for the analysis of axially loaded piles, Proceedings of the International Workshop on Recent Advances in Deep Foundations (IWDPF07). Ed. by Kikuchi, Otani, Kimura and Morikawa.
49. Seo, H. and Prezzi, M. (2007). Analytical solutions for a vertically loaded pile in multilayered soil. Geomechanics and Geoengineering: An International Journal, 2 (1), pp 51-60.

50. Seo, H., Basu, D., Prezzi, M and Salgado, R. (2009). Load-settlement response of rectangular and Circular piles in multilayered soil. Journal of Geotechnical and Geoenvironmental Engineering, 135 (3), pp 420-430.
51. Skipper, J., Follet, B., Menkiti, C. O, Long, M. and Clarke-Hughes, J. (2005). The engineering geology and characterisation of Dublin Boulder Clay. Q. J. Engng Geol. Hydrogeol. 38, No. 2, 171–187.
52. Trochanis, A.M., Bielak, J. and Christiano, P. (1991). Three-dimensional nonlinear study of piles. Journal of Geotechnical Engineering, American Society of Civil Engineers, 117 (3), pp 429-447.
53. Vallabhan, C. V. G. and Das, Y. C. (1991a). Modified Vlasov model for beams on elastic foundations. Journal of Geotechnical Engineering, American Society of Civil Engineers, 117(6), pp 956-966.
54. Vallabhan, C.V.G. and Mustafa, G. (1996). A new model for the analysis of settlement of drilled piers. International Journal of Numerical and Analytical Methods in Geomechanics, 20, pp 143-152.
55. Verruijt, A. and Kooijman, P. A. (1989). Laterally Loaded Piles in a Layered Elastic Medium. Géotechnique, 39(1), pp 39-46.
56. Vlasov, V. Z and Leont'ev, N. N. (1966). Beams, plates and shells on elastic foundations. Jerusalem: Israel Program for Scientific Translations.
57. Vucetic, M. (1994). Cyclic threshold shear strains in soils. Journal of Geotechnical and Geoenvironmental Engineering, 120 (12), pp 2208-2228.
58. Yamashita, S., Hori, T. and Suzuki, T. (2003). Effects of fabric anisotropy and stress condition on small strain stiffness of sands. Proceedings of the Deformation Characteristics of Geomaterials, 1, pp 187-194. (Proc. Lyon), Swets and Zeitlinger, Lisse.